^{2}H(d,γ)^{4}He reaction from a microscopic point of view

A. Arriaga, A. M. Eiró, and F. D. Santos
Centro de Física Nuclear da Universidade de Lisboa, Portugal

J. E. Ribeiro
Centro de Física da Matéria Condensada, Lisboa, Portugal
(Received 12 November 1987)

A microscopic study of the ^{2}H(d,γ)^{4}He reaction with deuteron and ^{4}He bound state wave functions which include the D-state components is presented. Cross section and tensor analyzing powers are calculated for deuteron energies between 1 and 15 MeV. Deuteron D-state effects are found to be particularly important in the transition amplitude arising from the $^5S_2$ scattering state. A detailed comparison between cluster and microscopic calculations is presented. Using an effective two-body model the analysis of A_{yy} data, in the energy range $1 \leq E_d \leq 15$ MeV, gives for the asymptotic D/S state ratio in ^{4}He the value $\rho = -0.18$.

I. INTRODUCTION

In the last few years there has been an increased interest in the experimental and theoretical study of the ^{2}H(d,γ)^{4}He reaction. Measurements of cross section and polarization observables have been carried out for deuteron energies ranging from 50 keV to 95 MeV.[1-4] At very low energies the radiative fusion of two deuterons is a process that may be of significant importance in astrophysics, since it may have an effect on the predicted abundances of the very light elements in the Universe.[5] Detailed knowledge of this reaction is also significant in view of the possible applications in fusion research.[6] The ^{2}H(d,γ)^{4}He reaction can also be used as a tool to study the structure of the ^{4}He, particularly its D-state component which is generated by the tensor force term of the N-N interaction.

An important aspect of the mechanism of this capture reaction is that the identity of the two deuterons in the entrance channel restricts the scattering states $^{2s+1}l_J$ to those where l and s have the same parity. For electromagnetic multipoles with $L \leq 2$ the allowed transitions are[7] $(E1;^3P_1)$, $(M1;^5D_1)$, $(E2;^1D_2)$, $(E2;^5S_2)$, $(E2;^5D_2)$, $(E2;^5G_2)$, $(M2;^3P_2)$, and $(M2;^3F_2)$. Considerations based on isospin conservation indicate that the $E2$ capture is expected to be dominant. Assuming a direct capture model for the reaction, we have shown[8] that both the tensor analyzing powers (TAP), and the cross section $\sigma(\theta)$ at very low energies are sensitive to the α-particle D state. In this cluster approximation, characterized by a point deuteron model for the electromagnetic operator, the structure of the deuterons and of the ^{4}He come into the transition amplitudes only through the overlap $\langle \phi_d^{\sigma_{13}} \phi_d^{\sigma_{24}} | \phi_\alpha^0 \rangle$, which contains both S and D-state components in $\mathbf{r}$, the separation coordinate of the two deuterons in ^{4}He. Since the $E2$ operator is proportional to r^2, the calculated amplitudes probe the asymptotic region of the wave functions. A strong sensitivity to ρ—the D/S state ratio in the d + d configuration of ^{4}He—was consequently observed in the TAP for 2 MeV $\leq E_d \leq$ 15 MeV, and in the cross section for $E_d \leq 2$ MeV.[8] It was then suggested that the reaction could be used in an empirical way of determining ρ through measurements of $\sigma(\theta)$, or through measurements of A_{yy}. The latter observable is preferred since it is the TAP which is less dependent on the initial state interactions. However, the analysis of $\sigma(\theta)$ and A_{yy} data suggests different values for ρ, -0.2, and -0.1, respectively. This discrepancy can be interpreted as an indication that the reaction mechanism is more complicated than the simple direct radiative capture model that was initially proposed. It should be emphasized that the values of the ^{4}He D-state probability, P_D, inferred from the comparison between theoretical calculations and experimental data is more model dependent than ρ, since the capture reaction at low energy is very sensitive to the asymptotic region of the bound state wave function.

In recent theoretical[9] and experimental[10] work, multipoles other than $E2$ were considered. The effect of the inclusion of $E1$, $M1$, and $M2$ was studied in the analyzing powers. Clear evidence was found for the admixture of an odd parity multipole, either $E1$ (where the contribution arises from the spin dependent part of the operator) or $M2$. Nevertheless, it remains unclear which multipoles account for the data. While the $E1$ and $M2$ transitions are crucially important to explain the A_y data, it was shown that they have only minor effects in the cross section and in the tensor analyzing powers. This is a consequence of angular momentum selection rules and can be understood as follows: (i) No spin tensors of rank one can be constructed from the interference of the dominant $E2$ amplitude—$(E2;^1D_2)$—and the remaining $E2$ amplitudes $(E2;^5S_2)$, $(E2;^5D_2)$, and $(E2;^5G_2)$. Therefore, the normally most important interference terms do not contribute to A_y. (ii) No spin tensors of rank zero or two can arise from the interference of $E1$ or $M2$ with the dominant $E2$ transition–$(E2;^1D_2)$. Thus, these interference terms do not contribute to either the cross section or

the TAP. The $E1$ and $M2$ multipoles can also play an important role whenever the ($E2;^1D_2$) contribution becomes very small. This occurs for instance in the angular distribution of all the observables in the region close to $\theta=\pi/2$.

Our main objective in the present paper is to analyze the ^{2}H(d,γ)^{4}He reaction from a microscopic point of view using ^{4}He and deuteron bound state wave functions which include both the S- and D-state components. We will restrict our study to the contribution of the $E2$ multipole to the cross section and TAP.

In Sec. II we describe the full microscopic $E2$ operator and its matrix elements. Section III deals with an analytical method used to calculate the $E2$ matrix elements between states expanded in an harmonic oscillator basis.

II. FORMALISM

In first order perturbation theory the interaction Hamiltonian for the emission of a photon with momentum $\mathbf{k}$ and polarization $\boldsymbol{\varepsilon}_n$ is given in the notation of Rose and Brink[11] by the expression

$$H_e(\mathbf{k},\boldsymbol{\varepsilon}_n)=-\sum_{LM\pi} n^{\pi} T^{+}_{LM}(\pi) D^{L}_{Mn}(R)^{*} , \tag{1}$$

where $\pi=0$ and 1 correspond to electric and magnetic operators, respectively, R is a rotation taking the z axis into the direction of $\mathbf{k}$. We use the Madison convention coordinate system where the z axis is along the momentum $\mathbf{p}$ of the incident particle and the y axis is along $\mathbf{p}\times\mathbf{k}$. The $T_{LM}(\pi)$ are multipole operators of rank L and are given by sums over all nucleons of one body operators Q'_{LM}, Q_{LM}, M_{LM}, M'_{LM} defined in Ref. 11. We have

$$T_{LM}(0)=\alpha_L(0)\sum_j [Q_{LM}(\mathbf{r}_j)+Q'_{LM}(\mathbf{r}_j)] , \tag{2}$$

$$T_{LM}(1)=\alpha_L(1)\sum_j [M_{LM}(\mathbf{r}_j)+M'_{LM}(\mathbf{r}_j)] , \tag{3}$$

where $\mathbf{r}_j$ is the position of the jth nucleon relative to the center of mass (c.m.) of the system and

$$\alpha_L(0)=\frac{(ik)^L}{(2L-1)!!}\left[\frac{L+1}{2L}\right]^{1/2} , \tag{4}$$

$$\alpha_L(1)=-i\alpha_L(0) . \tag{5}$$

In the long wavelength approximation (LWA), we have

$$Q_{LM}(\mathbf{r}_j)=-2e_j\mu_N\frac{i}{k}\left[\frac{4\pi}{2L+1}\right]^{1/2}\nabla_j[r_j^L Y_{LM}(\hat{\mathbf{r}}_j)]\cdot\mathbf{p}_j , \tag{6}$$

where $e_j=\frac{1}{2}[1+T_z(j)]$ and ∇_j and $\mathbf{p}_j$ are gradient and linear momentum operators for nucleon j, μ_N is the nucleon magneton, and $T_z(j)$ is the z component of the isospin operator related to the jth particle. The spin dependent part of $T_{LM}(0)$, Q'_{LM}, is known to be negligible in this long wave length limit[11] and therefore we only consider the dominant part Q_{LM} which can be simplified to

$$T^{+}_{LM}(0)=\alpha_L(0)e\sum_j\left[\frac{4\pi}{2L+1}\right]^{1/2} e_j r_j^L Y^{*}_{LM}(\hat{\mathbf{r}}_j) , \tag{7}$$

where e is the elementary charge. Meson exchange currents are taken into account for the electric transitions within the LWA (Siegert's theorem).

We use a system of Jacobian coordinates defined by

$$\begin{aligned}\mathbf{r}_{13}&=(\mathbf{r}_1-\mathbf{r}_3)/\sqrt{2} ,\\ \mathbf{r}_{24}&=(\mathbf{r}_2-\mathbf{r}_4)/\sqrt{2} ,\\ \mathbf{r}&=[(\mathbf{r}_1+\mathbf{r}_3)-(\mathbf{r}_2+\mathbf{r}_4)]/2 ,\end{aligned} \tag{8}$$

where 1,2 and 3,4 stand for pairs of identical particles. Since only the isoscalar part of the multipole operator contributes, for the $E2$ transition Eq. (7) can be written in a convenient notation as

$$T^{+}_{2M}(0)=E^{[r]}_{2M}+E^{[13]}_{2M}+E^{[24]}_{2M} , \tag{9}$$

where

$$\begin{aligned}E^{[r]}_{2M}&=\alpha_2(0)e\left[\frac{4\pi}{5}\right]^{1/2}\tfrac{1}{2}r^2Y^{*}_{2M}(\hat{\mathbf{r}}) ,\\ E^{[13]}_{2M}&=\alpha_2(0)e\left[\frac{4\pi}{5}\right]^{1/2}\tfrac{1}{2}r_{13}^2Y^{*}_{2M}(\hat{\mathbf{r}}_{13}) ,\\ E^{[24]}_{2M}&=\alpha_2(0)e\left[\frac{4\pi}{5}\right]^{1/2}\tfrac{1}{2}r_{24}^2Y^{*}_{2M}(\hat{\mathbf{r}}_{24}) .\end{aligned} \tag{10}$$

Neglecting[12] the coupling between channels with different l and s the scattering state is given by

$$\langle \mathbf{r}_{13}\mathbf{r}_{24}\mathbf{r}\,|\,^{2s+1}l_J\rangle=\mathcal{A}\sum_{m\sigma}(lms\sigma\,|\,JM_J)[\phi_d(\mathbf{r}_{13})\phi_d(\mathbf{r}_{24})]^{s\sigma}\psi_{ls}(\mathbf{r}) , \tag{11a}$$

with

$$[\phi_d(\mathbf{r}_{13})\phi_d(\mathbf{r}_{24})]^{s\sigma}=\sum_{\sigma_{13}\sigma_{24}}(1\sigma_{13}1\sigma_{24}\,|\,s\sigma)\phi_d^{\sigma_{13}}(\mathbf{r}_{13})\phi_d^{\sigma_{24}}(\mathbf{r}_{24}) , \tag{11b}$$

where $\phi_d^{\sigma_{ij}}(r_{ij})$ are the deuteron wave functions. The radial wave functions $\psi_{ls}(\mathbf{r})$, which describe the relative motion of the two deuterons, were generated as in Ref. 1 assuming a two body scattering determined by separable potentials constrained to give the energy dependence of the phase shifts obtained by Chwieroth, Tang, and Thompson using the resonating group method.[13] This effective two-body model does not include the coupling to other partitions of the four-body system, and therefore does not satisfy the four-body unitarity. Coulomb effects

were estimated as in Ref. 1 using an energy dependent Coulomb transmission factor. Since the distortion is very weak in the $^5G_2$ channel, we describe the $\psi_{42}(r)$ wave function by a simple Coulomb function with $l=4$. In Eq. (11) $\mathcal{A}$ is the full antisymmetrization operator.

In order to study the sensitivity of the matrix elements to the description of the bound state using different wave functions, we carried out three microscopic calculations where the deuterons and alpha particles were represented differently. In calculation (1) we used for the deuterons harmonic oscillator functions for the S and D states, which reproduce the rms radius of 1.96 fm, and with a D-state probability that was varied between 4 and 7%. For the alpha particle S state we also used a Gaussian wave function fitted to the rms radius of 1.42 fm. The alpha particle D state $|\psi_\alpha^D\rangle$ was generated in a perturbative way from the S state $|\psi_\alpha^S\rangle$ and is given as[14]

$$|\psi_\alpha^D\rangle = N(1+P^{12})(V_T^{[13]}+V_T^{[24]})|\psi_\alpha^S\rangle , \tag{12}$$

where P^{12} is the exchange operator. To describe $V^{[ij]}$, the tensor interaction between nucleons i and j, we used the tensor part of one-pion exchange (OPE) interaction with the cutoff of Ref. 15 which corresponds to a πNN form factor. The normalization N was fixed under the condition that the overlap function gives the same ^{4}He D_2 parameter as Schiavilla *et al.*[16] corresponding to the Argonne ($D_2=-0.16$ fm^2) and Urbana ($D_2=-0.24$ fm^2) interactions.

In calculation (2) we improved the description of the deuterons using the wave function of Reid soft core (SC) (Ref. 17) while keeping the same wave function for the alpha particle. Finally, in calculation (3), we improved the description of the bound state of the α particle using an exponential wave function $\phi_\alpha = N_\alpha \exp[-\beta\xi]/\xi$, with $\xi^2=(r_{13}^2+r_{24}^2+r^2)$. The free parameter β was determined by the condition that the overlap $\langle \phi_d^{\text{Reid}}\phi_d^{\text{Reid}}|\phi_\alpha\rangle$ has the correct asymptotic behavior.

In all the calculations we neglect the second order effects corresponding to the terms involving simultaneously the D-state components of the α particle and the deuterons. In this framework the $E2$ reduced matrix elements of Eq. (7) are given by

$$A=\langle 0\|T_2^+\|^1D_2\rangle=\langle {}^1S_0\|E_2^{[r]}\|^1D_2\rangle = \frac{\sqrt{15}}{16\pi}\int U_0^*(r)\phi_{20}(r)r^4dr , \tag{13}$$

$$B=\langle 0\|T_2^+\|^5S_2\rangle = B1+B2+B3 , \tag{14a}$$

with

$$B1=\langle {}^5D_0\|E_2^{[r]}\|^5S_2\rangle = N\frac{\sqrt{15}}{80\pi}\int U_2^*(r)\psi_{02}(r)r^4dr , \tag{14b}$$

$$B2=\langle {}^5D_0\|E_2^{[13]}+E_2^{[24]}\|^5S_2\rangle = N\frac{\sqrt{3}}{\sqrt{20\pi}}\int [\tfrac{1}{2}F_0^*(r)+\tfrac{1}{2}G_0^*(r)]\psi_{02}(r)r^2dr , \tag{14c}$$

$$B3=\langle {}^1S_0\|E_2^{[13]}+E_2^{[24]}\|^5S_2\rangle = (\tfrac{3}{2})^{1/2}\int H_0^*(r)\psi_{02}(r)r^2dr , \tag{14d}$$

$$C=\langle 0\|T_2^+\|^5D_2\rangle = C1+C2 , \tag{15a}$$

with

$$C1=\langle {}^5D_0\|E_2^{[r]}\|^5D_2\rangle = -N\frac{(2\sqrt{15})}{16\pi\sqrt{14}}\int U_2^*(r)\psi_{22}(r)r^4dr , \tag{15b}$$

$$C2=\langle {}^5D_0\|E_2^{[13]}+E_2^{[24]}\|^5D_2\rangle = -N\frac{\sqrt{3}}{2\sqrt{14\pi}}\int G_2^*(r)\psi_{22}(r)r^2dr , \tag{15c}$$

$$D=\langle 0\|T_2^+\|^5G_2\rangle = D1+D2 , \tag{16a}$$

with

$$D1=\langle {}^5D_0\|E_2^{[r]}\|^5G_2\rangle = N\frac{9\sqrt{15}}{40\pi\sqrt{14}}\int U_2^*(r)\psi_{42}(r)r^4dr , \tag{16b}$$

$$D2=\langle {}^5D_0\|E_2^{[13]}+E_2^{[24]}\|^5G_2\rangle = N\frac{3\sqrt{6}}{4\sqrt{35\pi}}\int G_4^*(r)\psi_{42}(r)r^2dr . \tag{16c}$$

In these expressions $U_0(r)$, $U_2(r)$, $H_0(r)$, and $F_0(r)$ are, respectively, the radial part of the overlaps (17), (18), (19), and (20)

$$\langle \mathbf{r}[\phi_d\phi_d]^{s\sigma}|\psi_\alpha^s\rangle = \sum_{\sigma_{13}\sigma_{24}}(1\sigma_{13}1\sigma_{24}|s\sigma)\tfrac{1}{2}(-)^{1-\sigma_{13}}\delta_{\sigma_{13}-\sigma_{24}}U_0(r)Y_{00}(\hat{\mathbf{r}}) , \tag{17}$$

$$\langle \mathbf{r}[\phi_d\phi_d]^{s\sigma}|P^{12}(V_T^{[13]}+V_T^{[24]})|\psi_\alpha^s\rangle = \sum_{\sigma_{13}\sigma_{24}}(1\sigma_{13}1\sigma_{24}|s\sigma)\sum_{M'}\tfrac{1}{2}(-)^{1-\sigma_{13}}(2M'1\sigma_{24}|1-\sigma_{13})U_{2M'}(\mathbf{r}) , \tag{18a}$$

with

$$U_{2M'}(\mathbf{r})=U_2(r)Y_{2M'}(\hat{\mathbf{r}}) , \tag{18b}$$

$$\langle \mathbf{r}[\phi_d\phi_d]^{s\sigma}|(E_{2M}^{[13]}+E_{2M}^{[24]})|\psi_\alpha^s\rangle = \delta_{M\sigma}\delta_{2s}\left[\frac{F3}{20}\right]^{1/2}H_0(r)Y_{00}(\hat{\mathbf{r}}) , \tag{19}$$

$$\langle \mathbf{r}[\phi_d\phi_d]^{s\sigma} \mid (E_{2M}^{[13]}+E_{2M}^{[24]})(V_T^{[13]}+V_T^{[24]}) \mid \psi_\alpha^s\rangle = \sum_{\sigma_{13}\sigma_{24}} (1\sigma_{13}1\sigma_{24} \mid s\sigma) \sum_{M'} \tfrac{1}{2}\delta_{MM'}(-)^{1-\sigma_{13}}(2M'1\sigma_{24} \mid 1-\sigma_{13})F_0(r)Y_{00}(\hat{\mathbf{r}}) \ . \tag{20}$$

The functions $G_0(r)$, $G_2(r)$, and $G_4(r)$ are, respectively, the radial functions of the $L=0$, $L=2$, and $L=4$ components of the overlap

$$\langle \mathbf{r}[\phi_d\phi_d]^{s\sigma} \mid [(E_{2M}^{[13]}+E_{2M}^{[24]})P^{12}(V_T^{[13]}+V_T^{[24]})] \mid \psi_\alpha^s\rangle = \sum_{\sigma_{13}\sigma_{24}} (1\sigma_{13}1\sigma_{24} \mid s\sigma) \sum_{M'} \tfrac{1}{2}(-)^{1-\sigma_{13}}(2M'1\sigma_{24} \mid 1-\sigma_{13})G^{MM'}(\mathbf{r}) \ , \tag{21a}$$

with

$$G^{MM'}(\mathbf{r}) = \sum_{LM_L} (-)^N(2-M'LM_L \mid 2M')(20L0 \mid 20)G_L(r)Y_{LM_L}(\hat{\mathbf{r}}) \ . \tag{21b}$$

The overlaps that involve the exchange operator P^{12}, corresponding to Eqs. (18) and (21), were evaluated with the help of the graphical rules of Ref. 18 and are briefly outlined in the next section.

III. THE P^{12} TYPE MATRIX ELEMENTS

Let us consider Eqs. (18) that defines the function $U_{2M'}(\mathbf{r})$. Dropping the spin dependence, this overlap can be represented geometrically by the diagram

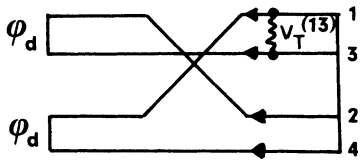

ψ_α + (insertion of $V^{[24]}$) . (22)

Expanding $V_T^{[ij]}\psi_\alpha$ and ϕ_d in an harmonic oscillator basis:

$$[V_T^{[ij]}\psi_\alpha(\mathbf{r}_{13}\mathbf{r}_{24}\mathbf{r})]_{2M'} = \sum_{n_1'n_2'n_3'} C_{n_1'n_2'n_3'}^{[ij]}\phi_{n_1'2M'}(\mathbf{r}_{ij})\phi_{n_2'00}(\mathbf{r}_{kl})\phi_{n_3'00}(\mathbf{r}) \ , \tag{23}$$

$$\phi_d(\mathbf{r}_{ij}) = \sum_{n_i} d_{n_i}\phi_{n_i00}(\mathbf{r}_{ij}) \ , \tag{24}$$

one can apply directly the graphical rules to Eq. (22) and get the coefficients u_{n_3} of the spectral decomposition of $U_{2M'}(\mathbf{r})$ in terms of $\phi_{n_32M'}(\mathbf{r})$, the harmonic oscillator wave function;

$$U_{2M'}(\mathbf{r}) = \sum_{n_3} u_{n_3}\phi_{n_32M'}(\mathbf{r}) \ , \tag{25}$$

where

$$u_{n_3} = u_{n_3}^{[13]} + u_{n_3}^{[24]} \ . \tag{26}$$

Figure 1 represents the general diagram involved in the calculation of the contribution to u_{n_3} arising from the first term in Eq. (22) which corresponds to the $V_T^{[13]}$ operator, identified as $u^{[13]}(n_1n_2n_3,n_1'n_2'n_3')$. In the notation $[n_il_im_i]$, n_i is the radial excitation and l_im_i the an-

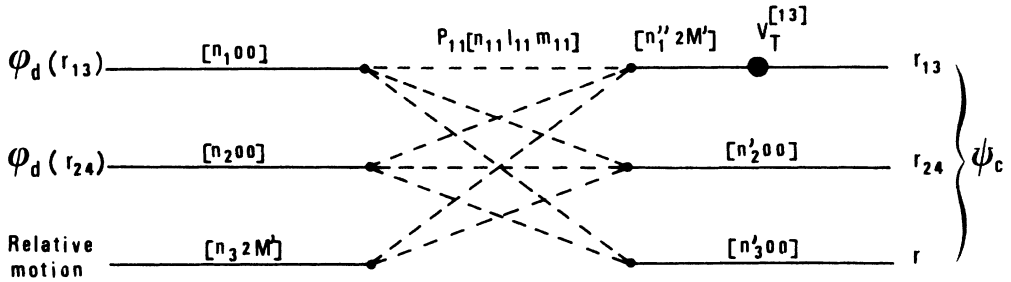

FIG. 1. General diagramatic representation of the coefficient u_{n_3} associated with the first term of Eq. (22). The absence of the P_{33} propagator is due to the fact that the matrix element $[P^{12}]_{33}$ is zero.

gular excitations associated with the expansions in the harmonic oscillator basis. The propagators (dashed lines) also carry excitations, $[n_{ij}l_{ij}m_{ij}]$ only shown in the figure for the P_{11} propagator. Conservation of harmonic oscillator energy $(2n+l)$ and angular momenta selection rules are assumed in each vertex, and a sum is worked out for all the intermediate states compatible with such constraints. Each propagator P_{ij} is proportional to

$$P_{ij} \propto [P^{12}]_{ij}^{2n_{ij}+l_{ij}} , \tag{27}$$

where $[P^{12}]_{ij}$ is the ij matrix element of the exchange operator in the system of Jacobian coordinates. The $u_{n_3}^{[13]}$ coefficient is then given by

$$u_{n_3}^{[13]} = \sum_{\substack{n_1 n_2 \\ n_1' n_2' n_3'}} u^{[13]}(n_1 n_2 n_3, n_1' n_2' n_3') C_{n_1' n_2' n_3'}^{[13]} \mathrm{d}_{n_1} \mathrm{d}_{n_2} . \tag{28}$$

The $u_{n_3}^{[24]}$ results from equivalent diagrams, as in Fig. 1, corresponding to the insertion of the $V_T^{[24]}$ operator, which represents the second term of Eq. (22).

The calculation of $G^{MM'}(\mathbf{r})$ defined in Eq. (21) is performed using the same procedure with the further inclusion of the $E_{2M}^{[ij]}$ operator in the deuteron lines. Hence, the expansion of $E_{2M}^{[ij]}\phi_{\mathrm{d}}^{s}$ in an harmonic oscillator basis is also required. As in the previous case, the graphical rules provide the coefficients of the decomposition of $G^{MM'}(\mathbf{r})$ in the harmonic oscillator basis:

$$G^{MM'}(\mathbf{r}) = \sum_{n_3 L M_L} (2M' L M_L \mid 2-M) \times (20L0 \mid 20) g_{n_3 L}(r) \phi_{n_3 L M_L}(\mathbf{r}) , \tag{29}$$

where the Clebsh-Gordon coefficients appear due to the presence of the E_{2M} operator which also carries an orbital angular momentum.

It should be stressed, that although the harmonic oscillator basis expansions

$$\langle n_i 00 \mid \phi_{\mathrm{d}}^{s} \rangle ; \langle n_i 2M \mid E_{2M} \phi_{\mathrm{d}}^{s} \rangle$$

and

$$\langle n_1 2M' \; n_2 00 \; n_3 00 \mid V_T \psi_{\alpha}^{s} \rangle$$

can display a rather slow convergence, the compact structure of P^{12} enforces a rapidly converging series for both $U_2(\mathbf{r})$ and $G(\mathbf{r})$.

IV. RESULTS AND DISCUSSION

The amplitude A corresponding to the transition from the $^1D_2$ scattering state is formally the same in cluster and microscopic calculations, since we neglected the second order terms that arise from the interference between the D-state components in the deuteron and ^{4}He wave functions. The cluster components of the other amplitudes correspond to the $E_2^{[r]}$ part of the $E2$ operator and were identified as $B1$, $C1$, and $D1$ in Sec. II, while the

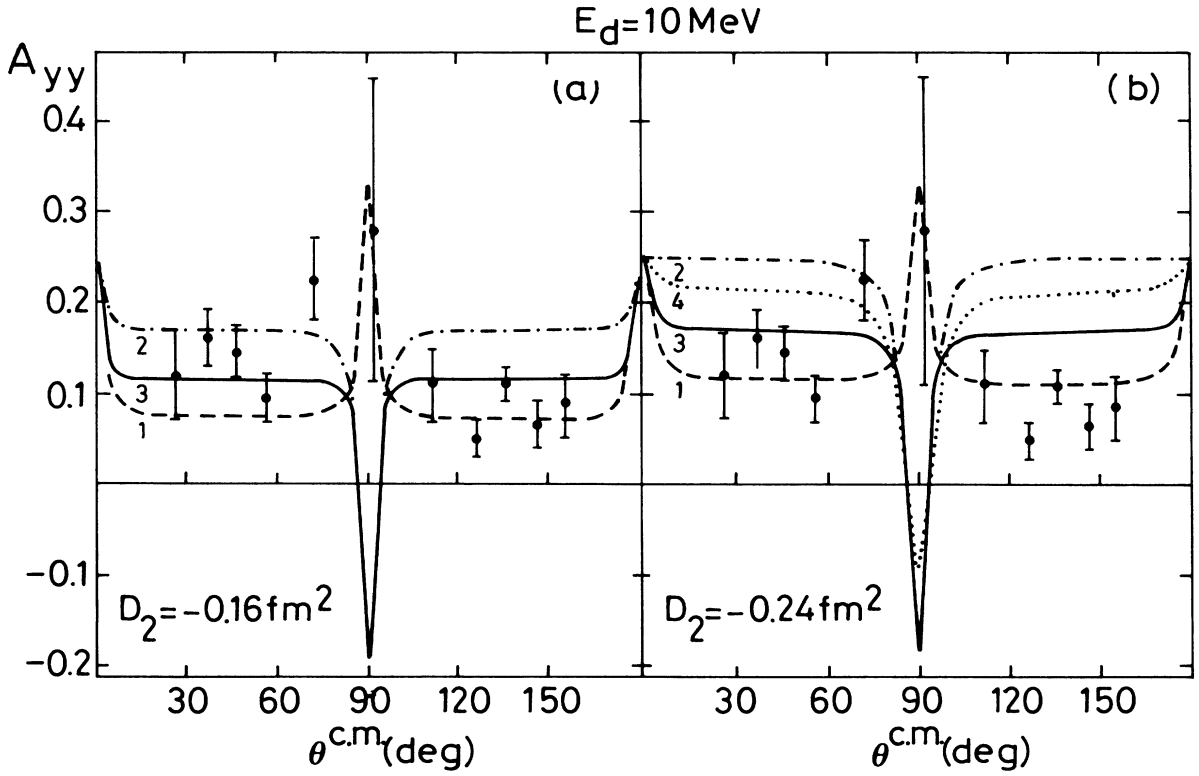

FIG. 2. Calculated tensor analyzing power $A_{yy}(\theta)$ for ^{2}H(d,γ)^{4}He reaction at $E_{\mathrm{d}} = 10$ MeV. The curves (1), (2), and (3) are the result of microscopic calculation explained in the text. Curve (4) is a cluster calculation from Ref. 8. The data are from Ref. 10.

microscopic components arising from $E\frac{1}{2}^{[13]}$ and $E\frac{1}{2}^{[24]}$ were identified as $B2$, $B3$, $C2$, and $D2$. The present calculations of the various contributions to the different $E2$ amplitudes were performed for deuteron energies between 1 and 15 MeV.

The microscopic effects in the amplitudes B, C, and D are very different. In the C amplitude the microscopic component expressed by the $C2$ term in Eq. (18) is of the order of 20% of the cluster component $C1$, while in the D amplitude this effect is of the order of 1%. The latter effect is a negligible correction because it arises from second order terms. The largest microscopic corrections are found in the B amplitude. In B there is a contribution from the $^5S_2 \rightarrow {}^1S_0$ transition which is generated from the interference between the deuteron D state and ^{4}He S state. This contribution, which corresponds to the $B3$ term defined in Eq. (14), is an S wave capture and therefore tends to become more important as the deuteron incident energy decreases. The effect of the deuteron D state is consequently enhanced at low energies. The other new contribution to B, namely $B2$, arises from a $^5S_2 \rightarrow {}^5D_0$ transition. The components of the $^5D_0$ wave function which contribute in each case are about the same order of magnitude, and consequently $B1$ and $B2$ are equally important in B. We find a strong destructive interference between the $^5S_2 \rightarrow {}^1S_0$ and $^5S_2 \rightarrow {}^5D_0$ transitions. Furthermore, due to large microscopic effects on the B amplitude, the quantity Re(B/A) is not proportional to ρ.

The calculated amplitudes A,B,C,D, including the microscopic contributions, were used to obtain angular distributions of the cross section and polarization observables. In Fig. 2 we show A_{yy} as a function of c.m. angle for an energy of 10 MeV. The dashed lines correspond to the use of harmonic oscillator wave functions for the deuterons and of a Gaussian function for the ^{4}He, and are referred as (1); the dash-dotted lines correspond to the use of the Reid soft core wave function for the deuterons and a Gaussian wave function for the ^{4}He, and are referred to as (2); the solid lines correspond to the use of the Reid soft core wave function for the deuteron and an exponential wave function for the ^{4}He and are referred to as (3). Figure 2(b) also shows the result of a cluster calculation from Ref. 8 performed with the Schiavilla wave function,[16] which is represented by the dotted line and referred to as (4). In the angular regions close to $\theta=\pi/4$ and $\theta=3\pi/4$, A_{yy} is approximately independent of B and proportional to Re(C/A).[7] The analysis of experimental A_{yy} data is therefore particularly suitable for the determination of ρ.

The inclusion of microscopic terms tends to lower the predicted value of A_{yy}, as it can be seen by the comparison of curves (3) and (4) in Fig. 2(b). This is a consequence of a destructive interference between the terms $C1$ and $C2$, which is analogous to that observed in the B amplitude. Consequently we conclude that the value of ρ extracted from cluster calculations is overestimated by about 20%. At $\theta=\pi/2$ we find that A_{yy} depends strongly on B, and therefore the predictions are very sensitive to the bound state wave functions used in the calculations. This sensitivity can be interpreted as a consequence of the node in the $^5S_2$ scattering state wave func-

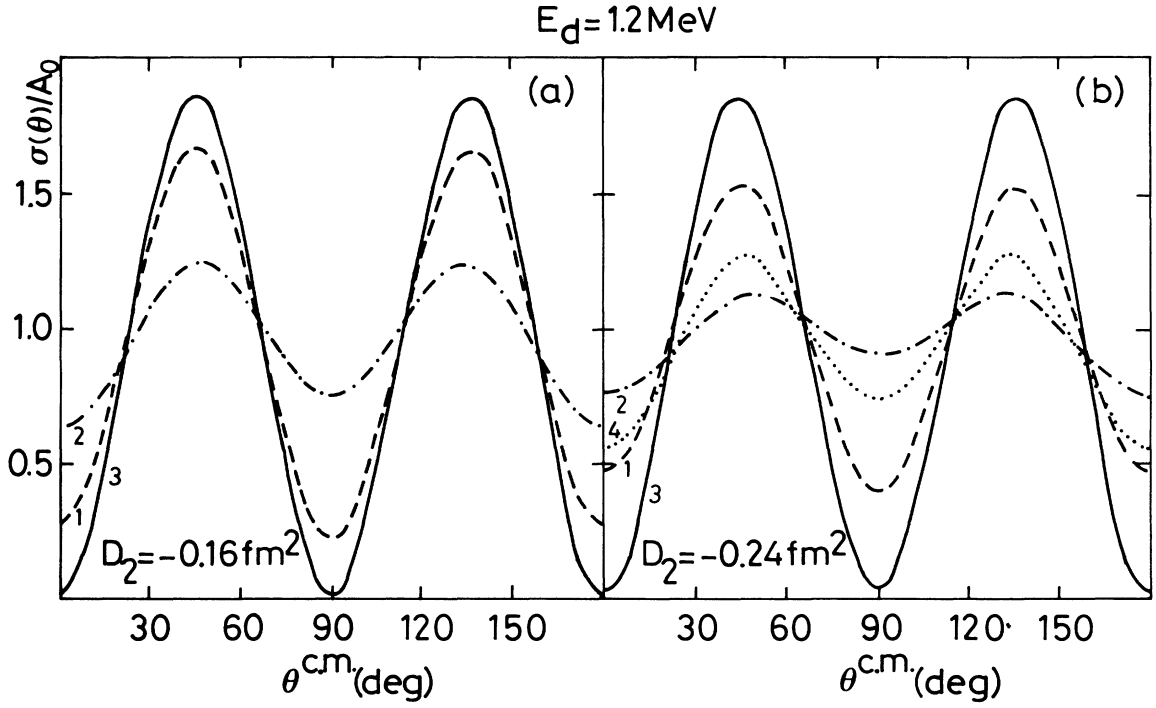

FIG. 3. Calculated differential cross section $\sigma(\theta)$ for the ^{2}H(d,γ)^{4}He reaction at $E_d = 1.2$ MeV. The curves have the same meaning as in Fig. 3 ($A_0 = \sigma_{tot}/4\pi$).

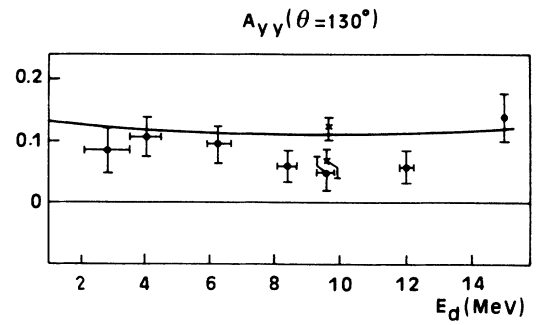

FIG. 4. Calculated tensor analyzing power A_{yy} for the reaction ^{2}H(d,γ)^{4}He for $\theta_{c.m.}=130°$ as a function of energy. The data were obtained in Tunl (●) and Wisconsin ($\times$) and are from Ref. 21. The curves is a result of calculation (3) described in the text corresponding to $D_2=-0.16$ fm^2.

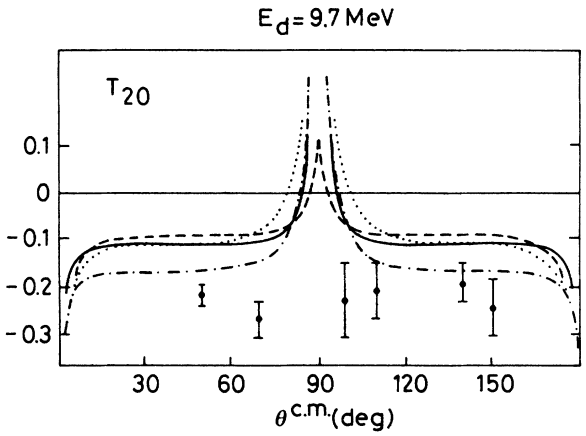

FIG. 5. Calculated tensor analyzing power T_{20} (θ) for ^{2}H(d,γ)^{4}He reaction at $E_d=9.7$ MeV. The dash, dash-dotted, and solid curves have the same meaning as in Fig. 3. The dotted line is a result of cluster calculation with a ^{4}He wave function of Ref. 16 corresponding to the Urbana interaction with $D_2=-0.24$ fm^2. The data are from Ref. 12.

tion, which in our model is associated with the strong Pauli repulsion. Even for a correct B amplitude, one cannot extract very meaningful information from A_{yy} at $\theta=\pi/2$ because the influence of multipoles other than $E2$ is of crucial importance in this angular region. The small asymmetries observed in the angular distribution of A_{yy} are associated with contributions from odd parity multipoles.

The sensitivity of the B amplitude to the use of different bound state wave functions can also be observed in Fig. 3 which shows the angular distribution of the cross section $\sigma(\theta)$ for $E_d=1.2$ MeV. The curves have the same meaning as in Fig. 2 and correspond to the three calculations mentioned. At this energy the cross section is almost entirely determined by the A and B amplitudes, and the comparison between experimental values and theoretical predictions of the ratio $R=\sigma(\pi/4)/\sigma(\pi/2)$ can provide information on the ratio $|A|/|B|$. At lower energies, below 0.3 MeV, the transition from the $^1D_2$ state tends to be inhibited[3] and the cross section becomes just a function of the B amplitude. The cluster description is then totally inadequate to describe the reaction and should not be used, even with the purpose of a qualitative discussion.[19] At these very low energies the description of the scattering state should account correctly for the Coulomb interaction since the use of penetration factors is no more a good approximation. Recently Assenbaum and Langanke,[20] considering spherical deuterons, estimated the D-state admixture in ^{4}He from a comparison between the results of a microscopic variational calculation and experimental data of $\sigma(\theta)$, for energies $E_d<0.3$ MeV. One should be aware that in this energy region to neglect the D state of the deuteron, and therefore the $^5S_2\rightarrow{}^1S_0$ transition, is a serious flaw in the extraction of reliable information about the ^{4}He D state.

In Fig. 4 we show the energy dependence of A_{yy} for $\theta=130°$. The curve is a result of calculation (3) described above, which is expected to be the most realistic since it ensures the good asymptotic behavior of the overlap functions. This calculation corresponds to a value of $D_2=-0.16$ fm^2 and therefore using the asymptotic approximation[22] $\rho=D_2\alpha^2$ (where α is the separation energy wave number) we obtain $\rho=-0.18$.

The present calculations do not yet provide a satisfactory explanation for T_{20}. This can be seen in Fig. 5 where the angular distribution of T_{20} for the various calculations described in the text are shown. This is again a signature of the importance of the B amplitude which is absent, in first order, in A_{yy}.

Recently Piekarewicz *et al.*[23] obtained $\rho\approx-0.40$ from a fit to cross section data at c.m. energies below 3 MeV, using a model where the scattering states as well as the components of the ground state of ^{4}He are assumed to be products of internal deuteron wave functions and a function of the relative motion. The effects of the deuteron D state were included through the quadrupole moment. However, we find that in order to account for these effects in the $^5S_2\rightarrow{}^1S_0$ transition, it is necessary to use a microscopic description with a realistic deuteron wave function. The very low value obtained for ρ in Ref. 23 is probably a consequence of the approximations involved in the inclusion of deuteron D-state effects.

The present results indicate clearly that microscopic calculations including deuteron D-state effects with a realistic deuteron wave function are essential to describe the transition from the $^5S_2$ scattering state. For a complete understanding of the mechanism of this reaction, a more consistent description of both scattering and bound state, satisfying four-body unitarity is required. Calculations including $E1$, $M1$, and $M2$ are in progress and will be reported elsewhere.

[1]H. R. Weller, P. Colby, J. Langerbrunner, Z. D. Huang, D. R. Tilley, F. D. Santos, A. Arriaga, and A. M. Eiró, Phys. Rev. C **34**, 32 (1986).

[2]F. J. Wilkerson III and F. E. Cecil, Phys. Rev. C **31**, 2036

(1985).
[3]C. A. Barnes, K. Chang, T. R. Donaghue, C. Rolfs, and J. Kammeraad, Phys. Lett. B **197**, 315 (1987).
[4]W. K. Pitts, Ph.D. thesis, University of Indiana, 1987 (unpublished).
[5]W. A. Fowler, Rev. Mod. Phys. **56**, 169 (1984); W. D. Arnett and J. W. Truran, *Nucleosynthesis—Challenges and New Developments* (University of Chicago Press, Chicago 1985).
[6]F. E. Cecil and D. E. Newman, Nucl. Instrum. Methods **221**, 449 (1984).
[7]F. D. Santos, A. Arriaga, A. M. Eiró, and J. A. Tostevin, Phys. Rev. C **31**, 707 (1985).
[8]A. Arriaga, A. M. Eiró, and F. D. Santos, in *Weak and Electromagnetic Interactions in Nuclei,* edited by H. V. Klapdor (Springer-Verlag, Heidelberg, 1986), p. 61.
[9]J. A. Tostevin, Phys. Rev. C **34**, 1497 (1986).
[10]S. Mellema, T. R. Wang, and W. Haeberli, Phys. Lett. **166B**, 282 (1986); Phys. Rev. C **34**, 2043 (1986).
[11]H. J. Rose and D. M. Brink, Rev. Mod. Phys. **39**, 306 (1967).
[12]H. R. Weller, P. Colby, N. R. Roberson, and D. R. Tilley, Phys. Rev. Lett. **53**, 1325 (1984).
[13]F. S. Chwieroth, Y. C. Tang, and D. R. Thompson, Nucl. Phys. **A189**, 1 (1972).
[14]A. D. Jackson and D. O. Riska, Phys. Lett. **50B**, 207 (1974).
[15]J. L. Friar, B. F. Gibson, and G. L. Payne, Phys. Rev. C **30**, 1084 (1984).
[16]R. Schiavilla, V. R. Pandharipande, and R. B. Wiringa, Nucl. Phys. **A449**, 219 (1986).
[17]R. V. Reid, Ann. Phys. **50**, 411 (1958).
[18]J. E. Ribeiro, Phys. Rev. D **25**, 2406 (1982); E. V. Beveren, Z. Phys. C **17**, 135 (1983).
[19]G. Bluge, H. J. Assenbaum, and K. Langanke, Phys. Rev. C **36**, 21 (1987).
[20]H. J. Assenbaum and K. Langanke, Phys. Rev. C **36**, 17 (1987).
[21]H. R. Weller, *Proceedings of the European Workshop on Few Body Physics,* edited by C. Ciotidegli Atti, O. Benhar, E. Pace, and G. Salmé (Springer-Verlag, Wien, 1986), Suppl. 1.
[22]B. C. Karp, E. J. Ludwig, J. E. Bowsher, B. L. Burks, T. B. Clegg, F. D. Santos, and A. M. Eiró, Nucl. Phys. **A457**, 15 (1986).
[23]J. Piekarewicz and S. E. Koonin, Phys. Rev. C **36**, 875 (1987).